

7-22-2003


## The structures of fluorene– (H<sub>2</sub>O)<sub>1,2</sub> determined by rotational coherence spectroscopy

David M. Laman

Alan G. Joly

Douglas Ray

Follow this and additional works at: <https://digitalcommons.cwu.edu/cotsfac>

 Part of the [Atomic, Molecular and Optical Physics Commons](#)

---

# The structures of fluorene-(H<sub>2</sub>O)<sub>1,2</sub> determined by rotational coherence spectroscopy

David M. Laman<sup>a)</sup>

*Department of Physics, Central Washington University, Ellensburg, Washington 98926-7422*

Alan G. Joly and Douglas Ray

*W. R. Wiley Environmental Molecular Sciences Laboratory, Pacific Northwest National Laboratory, Richland, Washington 99352*

(Received 27 December 1999; accepted 28 April 2003)

Rotational coherence spectroscopy (RCS), via time-correlated single photon counting, and two-color resonant two-photon ionization (R2PI) time-of-flight mass spectrometry, have been used to characterize fluorene-(water)<sub>1,2</sub> [FL-(H<sub>2</sub>O)<sub>1,2</sub>] van der Waals clusters generated in supersonic jets. Rotational coherence traces have been obtained at excitation energies corresponding to several resonant features in the  $S_1 \leftarrow S_0$  R2PI spectra of FL-(H<sub>2</sub>O)<sub>1,2</sub>. RCS simulations and diagonalization of the moment of inertia tensor have been used to obtain  $S_1$  excited state rotational constants and structures of FL-(H<sub>2</sub>O)<sub>1,2</sub> that are consistent with the experimental rotational coherence traces. The RCS results indicate that: (i) the water molecule in FL-H<sub>2</sub>O resides above the central five member ring and interacts with both aromatic sites; (ii) the water molecules in FL-(H<sub>2</sub>O)<sub>2</sub> form a water dimer that is most likely oriented along the long axis of fluorene and is hydrogen-bonded to both aromatic sites. The  $S_1 \leftarrow S_0$  R2PI spectra of FL-(D<sub>2</sub>O)<sub>1,2</sub> and FL-HDO have also been obtained. The  $0_0^0$  transition is a doublet in the R2PI spectra of FL-H<sub>2</sub>O, FL-D<sub>2</sub>O, and a singlet in the R2PI spectrum of FL-HDO. The presence of this doublet in the FL-H<sub>2</sub>O/D<sub>2</sub>O spectra, and the absence of such a splitting in the FL-HDO spectrum, is an indication of internal rotation of the water molecule on a potential energy surface that changes upon electronic excitation. Lastly, the use of RCS and time-resolved fluorescence as a tool for assigning features in R2PI spectra that are of ambiguous origin due to fragmentation of higher mass clusters into lower mass channels is demonstrated. © 2003 American Institute of Physics. [DOI: 10.1063/1.1584031]

## I. INTRODUCTION

Gas phase benzene-(water)<sub>n</sub> clusters have been the focus of a number of experimental<sup>1-11</sup> and theoretical<sup>8,12-16</sup> studies aimed at understanding the interaction between hydrogen bonding species and aromatic  $\pi$  systems. Benzene-(H<sub>2</sub>O)<sub>n</sub> complexes up to  $n=8$  and several isotopomers of the benzene-water complex have been studied with microwave,<sup>7,8</sup> partially rotationally resolved electronic absorption,<sup>9-11</sup> IR,<sup>1,3-5</sup> and Raman<sup>2</sup> spectroscopies. The major structural features of benzene-(water)<sub>n</sub> complexes deduced from these studies are as follows: (i) In the benzene-water complex, the water molecule interacts with the  $\pi$  cloud of benzene on or near the sixfold axis. Both water hydrogens participate in the interaction with benzene, although not to the same degree. (ii) Benzene-(H<sub>2</sub>O)<sub>n</sub> complexes with  $n \geq 2$  consist of hydrogen bonded networks of water molecules on one side of the benzene ring. The interaction of the water network with the  $\pi$  cloud of benzene is primarily through one OH group, and the hydrogen-bonded structure of the water network is only slightly perturbed by the benzene molecule.

Since the water-water binding energy additionally stabilizes benzene-(water)<sub>n>1</sub>, the above-summarized result (ii)

is not unexpected, i.e., the lowest energy configuration will have as many water-water hydrogen bonds as the free water cluster. Water molecules bound to opposite faces of the benzene ring cannot hydrogen bond, and thus such structures do not form. In aromatic systems more complex than benzene, however, the binding of water molecules to adjacent aromatic sites does not necessarily preclude water-water hydrogen bonding, and hence structures with networks of hydrogen-bonded water molecules bound to multiple aromatic sites can occur. A complete picture of the interaction of water with aromatic systems will thus require structural information on complexes of water with molecules containing multiple aromatic sites. Detailed structural information on such systems is currently limited to 9,9'-bifluorenyl-H<sub>2</sub>O (Ref. 17) and perylene-H<sub>2</sub>O,<sup>18</sup> both of which have been studied by rotational coherence spectroscopy (RCS).

Since its introduction by Felker, Baskin, and Zewail,<sup>19,20</sup> RCS has been used to determine the structures of a plethora of jet-cooled molecular complexes.<sup>17,18,21-27</sup> In RCS, a subset of rovibronic states is coherently populated by a linearly polarized picosecond laser pulse. The rotational quantum beats resulting from the time evolution of these coherently populated states can be monitored by a number of different techniques.<sup>27</sup> Information on the rotational energies, and hence the rotational constants, is contained in the temporal positions and separations of the rotational quantum beats,

<sup>a)</sup> Author to whom correspondence should be addressed. Electronic mail: lamand@cwu.edu

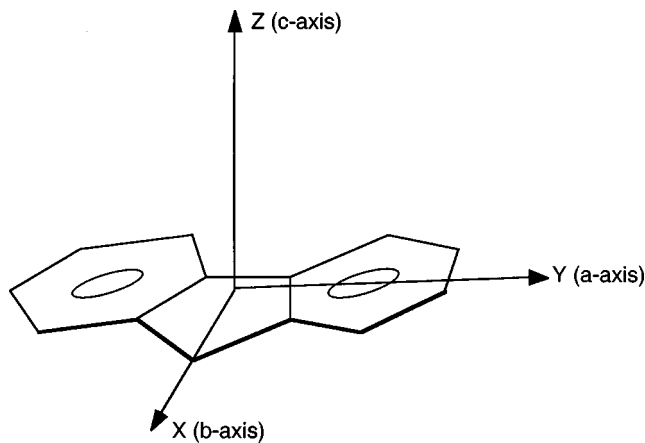


FIG. 1. Fluorene and its principal axis system.

and the rotational constants yield structural information via the principal moments of inertia.

We report here the structures of jet-cooled fluorene-(H<sub>2</sub>O)<sub>1,2</sub> [FL-(H<sub>2</sub>O)<sub>1,2</sub>] obtained from  $S_1$  excited state rotational constants measured by RCS via polarized time-resolved fluorescence. Fluorene (shown with its principal axis system in Fig. 1) is a useful molecule for studying complexes of water with molecules containing two adjacent aromatic sites. The fluorescence quantum yield (0.8)<sup>28</sup> of fluorene is fairly large, permitting the use of fluorescence techniques with good signal-to-noise, and its  $S_1 \leftarrow S_0$  absorption wavelength ( $\lambda_{0,0} \approx 296$  nm) is easily accessible with frequency doubled dye lasers. In addition, the *a*-type (parallel)  $S_1 \rightarrow S_0$  transition moment and rotational symmetry of fluorene makes it well suited for RCS studies. Jet-cooled clusters of fluorene with water have been previously studied by mass-resolved resonant two-photon ionization (R2PI),<sup>29</sup> dispersed emission spectroscopy,<sup>29</sup> and laser induced fluorescence,<sup>30</sup> however, no detailed experimental structural information on these clusters is available prior to the present study.

The  $S_1 \leftarrow S_0$   $0_0^0$  excitation energies used for RCS were determined with mass-resolved R2PI. Despite the ability of R2PI to provide mass resolution for cluster studies, ambiguities as to the mass origins of features in the R2PI spectra of weakly bound clusters frequently arise. The stable geometries of neutral clusters involving polar species such as FL-(H<sub>2</sub>O)<sub>*n*</sub> become energetically unfavorable upon ionization of the aromatic moiety since the attractive negative charge distribution necessary for hydrogen bonding is replaced with a repulsive positive charge distribution. Such ionized hydrogen-bonded clusters frequently fragment before rearrangement of the cluster into an energetically stable geometry can take place, complicating R2PI spectra taken in lower mass channels with resonant features due to fragmentation of higher mass species. Even though fragmentation efficiencies can be minimized by limiting the ionization photon energy to just above the ionization threshold, in general fragmentation cannot be completely eliminated. In such cases, complementary techniques that can aid in the identification of R2PI features can prove extremely useful. While RCS is valuable as a stand-alone technique, it can also be

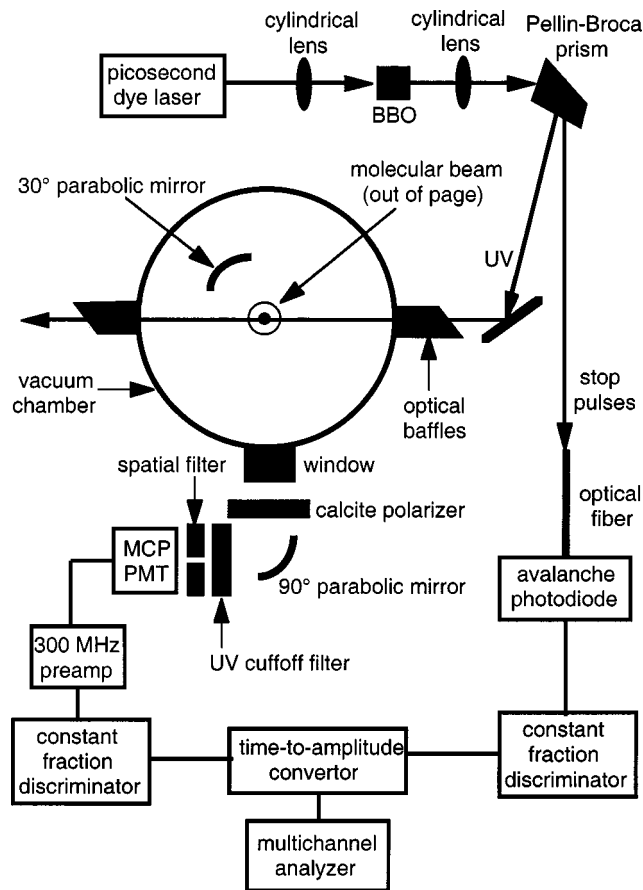


FIG. 2. Time-resolved fluorescence instrument for RCS of jet-cooled clusters.

used as an aid in the identification of R2PI features: R2PI features due to the same species will have the same rotational coherence traces; R2PI features due to different species will have different rotational coherence traces; and R2PI features due to multiple species will have rotational coherence traces with multiple sets of rotational recurrences each corresponding to a specific species (provided that all sets of recurrences are temporally resolved). In addition, structural information obtained from RCS can be used to tentatively assign R2PI features to specific species. In the present study, the RCS data have proven to be valuable in the interpretation of the R2PI spectra.

## II. EXPERIMENT

The experimental setup for RCS of FL-(H<sub>2</sub>O)<sub>*n*</sub> clusters by polarized time-resolved fluorescence is shown schematically in Fig. 2. Helium is bubbled through a thermostated cell containing deionized water, and the resulting He/water mixture is passed through an oven containing fluorene maintained at 70–90 °C. The resulting He/water/fluorene mixture is expanded through a 500- $\mu$ m-diam circular aperture into a chamber maintained at an operating pressure of approximately 0.15 Torr by an 800 l/s Roots pump system. The helium stagnation pressure is 2 atm.

The supersonic jet is crossed at a distance of 15 mm from the expansion aperture by linearly polarized ps UV pulses tuned to the  $S_1 \leftarrow S_0$  transition of FL-(H<sub>2</sub>O)<sub>*n*</sub> ( $\sim 296$

nm). The UV pulses are generated by frequency doubling in BBO the output of a cavity dumped (4.8 MHz) R6G dye laser (Coherent 700). An intracavity thin etalon is used to narrow the spectral width of the dye laser output to less than  $2\text{ cm}^{-1}$ , and to provide stabilization and fine adjustment ( $1\text{--}2\text{ cm}^{-1}$ ) of the laser frequency. The UV light is collimated before entering the chamber and the UV power is typically 1.5 mW. The residual fundamental light is separated from the second harmonic by a Pellin–Broca prism, and is directed by an optical fiber onto an avalanche photodiode for generation of the stop pulses for time-correlated single photon counting.

The UV input and output ports of the chamber are extensively baffled to minimize the background due to scattering. Fluorescence from the excitation region is collected, collimated, and directed out of the chamber by an  $f/2\ 30^\circ$  off-axis parabolic mirror, and is polarized by a large-aperture calcite polarizer oriented parallel to the polarization of the UV pulses. A  $90^\circ$  off-axis parabolic mirror focuses the polarized collimated fluorescence onto a microchannel plate photomultiplier tube (MCP PMT, Hamamatsu R3809U). The MCP PMT is covered with a 2-mm-thick UG11 cut-off filter in order to minimize background from room lights and scattered fundamental light from the dye laser. An  $800\text{-}\mu\text{m}$ -wide rectangular spatial filter in front of the MCP PMT blocks out the fringes of the image of the fluorescence region where the image quality is poor enough to degrade the time resolution of the instrument. The detection system is isolated from ambient light with a light-tight hood. Background counts rates are typically  $10\text{--}20\text{ s}^{-1}$ .

The output pulses from the MCP PMT and avalanche photodiode are amplified, discriminated, and used as the start and stop triggers, respectively, of a time-to-amplitude converter (TAC, Tennelec 864). The output pulses of the TAC are binned according to pulse height by a multichannel analyzer (MCA, Oxford), yielding a histogram of counts versus photon arrival time. Fluorescence count rates of well above  $50\,000\text{ s}^{-1}$  are easily obtained for FL–H<sub>2</sub>O, while fluorescence count rates for FL–(H<sub>2</sub>O)<sub>2</sub> were in the range  $2000\text{--}20\,000\text{ s}^{-1}$ . Counts were accumulated until no appreciable improvement in the signal-to-noise was observed. The counting times varied from 8 to 10 h for clusters with the lowest count rates to 1–2 h for clusters with the highest count rates.

The instrument response was determined by time-correlated single photon counting of Rayleigh scattering from air in the vacuum chamber at atmospheric pressure. The temporal width of the instrument response curve obtained in this manner is  $\sim 30\text{ ps}$  full width at half maximum (FWHM), which is adequate time resolution for RCS.

The MCA time-per-channel ( $6.393\text{ ps/channel}$ ) was calibrated by introducing known delays into the optical path of the UV pulses and measuring the change in MCA channel position of the peak of the instrument response curve as a function of delay time. The time per channel was found to be highly linear over the time range of interest. Corrections for the speed of light in air were included in the time per channel calibration, however, they introduce a rather small ( $0.03\%$ ) correction to the time per channel.

The time-of-flight reflectron mass spectrometer used in

the two-color R2PI studies is described in detail elsewhere.<sup>31</sup> FL–(H<sub>2</sub>O)<sub>*n*</sub> clusters for R2PI are produced by the above-described method in a pulsed expansion ( $750\text{-}\mu\text{m}$ -diam circular aperture) operated at 10 Hz with an  $80\ \mu\text{s}$  pulse width. A mixture of 90% Ne/10% He at 2 atm is used as the seed gas. The expansion is skimmed downstream from the nozzle with a 1-mm-diam conical skimmer. The position of the expansion aperture is adjustable so that the skimmer samples the coldest part of the expansion. In this way, two-color R2PI spectra for the  $0_0^0$  transition of bare fluorene with  $1.1\text{ cm}^{-1}$  FWHM and signal-to-noise ratios in excess of 100 ( $0.1\ \mu\text{J}$  resonant beam,  $100\ \mu\text{J}$  ionization beam) are routinely obtained.

The R2PI resonant beam (scanned around the  $S_1 \leftarrow S_0\ 0_0^0$  transition of the cluster) is the frequency doubled (KDP) output of a 10 Hz ns OPO (Spectra-Physics MOPO,  $0.2\text{ cm}^{-1}$  spectral width), and the ionization beam for ionization (continuum  $\leftarrow S_1$ ) is the frequency doubled output of a 10 Hz ns DCM dye laser. Both beams cross the molecular beam at right angles, are carefully overlapped in the interaction region, and are temporally synchronized with each other and the molecular beam. The resonant and ionization beams are focused into the interaction region with 75 and 100 cm focal length lenses, respectively. Pulse energies are typically  $0.1\text{--}0.5\ \mu\text{J}$  for the resonant beam and  $100\text{--}300\ \mu\text{J}$  for the ionization beam.

All the wavelengths quoted in the following were measured with a calibrated wavemeter (Burleigh WA-4000) and are referenced to vacuum.

### III. RESULTS

#### A. Assignment of the RCS spectra and R2PI features to specific species

A mass-resolved spectroscopic technique such as R2PI is required in order to determine the  $S_1 \leftarrow S_0$  excitation energies for RCS of clusters. The  $n=1,2$  mass channel two-color R2PI spectra of FL–(H<sub>2</sub>O)<sub>*n*</sub> in the spectral region around the origin transition of FL–H<sub>2</sub>O are shown in Fig. 3. A low ionization photon energy ( $\sim 30\,800\text{ cm}^{-1}$ ) was used in order to minimize cluster fragmentation. The spectral region shown is well to the blue of the  $S_1 \leftarrow S_0\ 0_0^0$  transition of bare fluorene ( $33\,776.0\text{ cm}^{-1}$ ). Rotational coherence traces have been obtained at excitation energies  $33\,849.4$ ,  $33\,838.0$ ,  $33\,833.4$ , and  $33\,827.0\text{ cm}^{-1}$  (labeled I–IV, respectively, in Fig. 3) corresponding to major features in the R2PI spectra. These rotational coherence traces are shown in Fig. 4.

The alternating polarity, uniformly spaced recurrences in the rotational coherence traces are identified as *J*-type recurrences. The vast majority of the features present are assigned as such. These recurrences are due to rotational quantum beats between states with  $\Delta J = \pm 1, 2$  and  $\Delta K = 0$ . For a prolate symmetric top, *J*-type recurrences are equally spaced at times  $\tau_n$  given by  $\tau_n = n/2(B+C)$ , where *n* is the recurrence number and *B*, *C* are the nonunique rotational constants of the rotor. For a near-prolate symmetric rotor,  $\tau_n = n/2(B+C)$  approximately holds, and a plot of  $1/\tau_n$  versus *n* will have a slope approximately equal to  $(B+C)/2$ . RCS traces obtained at wavelengths labeled I–III show no obvious

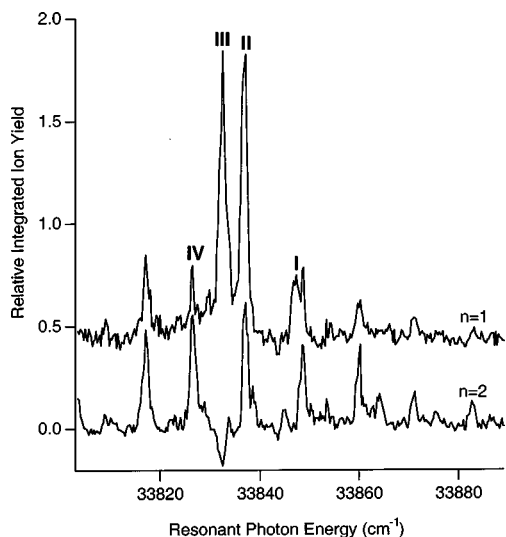


FIG. 3. Two-color R2PI spectra (ionization photon energy  $\sim 30\,800\text{ cm}^{-1}$ ) of fluorene-(H<sub>2</sub>O)<sub>n</sub>,  $n = 1, 2$ . Fragmentation of fluorene-(H<sub>2</sub>O)<sub>2</sub> into the  $n = 1$  mass channel is apparent in features I, II, IV.

C-type recurrences at times approximately equal to  $n/4C$ , suggesting that the species are very close to prolate symmetric.<sup>32</sup> However, RCS traces obtained upon laser excitation tuned to  $33\,827.0\text{ cm}^{-1}$  (IV) demonstrate clear C-type recurrences in addition to the numerous prominent J-type features. The existence of C-type recurrences implies a significant lowering of the symmetry of the species and provides additional information about the C rotational constant.

In practice, the experimental traces thus obtained are smoothed and then fit to a single exponential decay. The weighted residuals of these fits, which contain the rotational coherence features independent of the fluorescence decay, are used for determination of the recurrence times and for comparison to simulations. Plots of  $1/t_n$  versus  $n$  for the rotational coherence traces taken at all the aforementioned

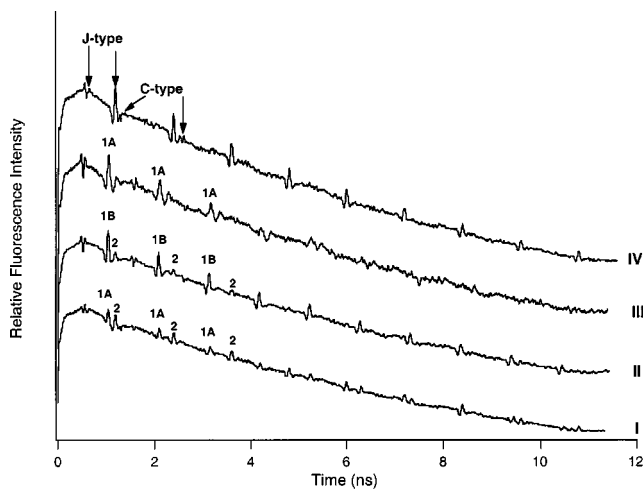


FIG. 4. Rotational coherence traces taken at excitation energies corresponding to features I–IV in the R2PI spectra of fluorene-(H<sub>2</sub>O)<sub>1,2</sub>–I ( $33\,849.4\text{ cm}^{-1}$ ): fluorene-H<sub>2</sub>O (1A) and fluorene-(H<sub>2</sub>O)<sub>2</sub> (2) in approximately equal proportions; II ( $33\,838.0\text{ cm}^{-1}$ ): fluorene-H<sub>2</sub>O with minor contribution from fluorene-(H<sub>2</sub>O)<sub>2</sub> (2); III ( $33\,833.4\text{ cm}^{-1}$ ): fluorene-H<sub>2</sub>O; IV ( $33\,827.0\text{ cm}^{-1}$ ): fluorene-(H<sub>2</sub>O)<sub>2</sub>.

TABLE I. Summary of RCS and  $S_1$  lifetime data.

Species	$B + C$ (GHz)	$S_1$ lifetime (ns)
fluorene	1.0572 <sup>a</sup>	15.6 <sup>b</sup>
fluorene <sup>c</sup>	$1.0568 \pm 0.0036$	$14.2 \pm 0.3$
FL-H <sub>2</sub> O (II)	$0.9562 \pm 0.0026$ (1B)	$12.4 \pm 0.2$
FL-H <sub>2</sub> O (III)	$0.9460 \pm 0.0075$ (1A)	$13.2 \pm 0.3$
	$0.9280 \pm 0.0060$ <sup>c</sup>	
FL-H <sub>2</sub> O (I)	$0.9452 \pm 0.0045$ (1A)	$12.7 \pm 0.3$ <sup>d</sup>
FL-(H <sub>2</sub> O) <sub>2</sub> (I)	$0.8294 \pm 0.0023$ (2)	$10.3 \pm 0.2$ <sup>d</sup>
FL-(H <sub>2</sub> O) <sub>2</sub> (IV)	$0.8298 \pm 0.0023$	$10.5 \pm 0.2$
FL-D <sub>2</sub> O (II)	$0.9450 \pm 0.0027$	
FL-D <sub>2</sub> O (III)	$0.9480 \pm 0.0027$	
FL-(D <sub>2</sub> O) <sub>2</sub> (IV)	$0.8131 \pm 0.0023$	

<sup>a</sup>Reference 20.

<sup>b</sup>Reference 15.

<sup>c</sup>This work.

<sup>d</sup>Result of biexponential fit.

<sup>e</sup>Minority component.

excitation energies are highly linear, indicating rotors that are very close to being symmetric. Still, due to the small asymmetry of the rotor, the values of  $B + C$  obtained from these plots supply only an approximate value which must be further refined using numerical simulations. The values of  $B + C$  obtained from RCS traces at each wavelength are tabulated in Table I along with assignments (discussed in the following) of the species associated with each trace.

The values of  $B + C$  obtained from RCS traces I–IV indicate that: (i) the J-type recurrences in trace IV and the features labeled 2 in trace I and trace II are due to the same species; (ii) the features labeled 1A in trace I and trace III are likely the same species; (iii) the predominant species in trace II labeled 1B is distinctly different ( $\sim 1\%$ ) from those labeled 1A in other traces. Trace III also contains additional features which are similar to but slightly different from those labeled 1A. At present, the assignment of these features is unclear. It is possible that this species is a minority isomer of FL-H<sub>2</sub>O, the smaller value of  $B + C$  implies that the water is significantly more displaced from the plane of the fluorene ring. We note that these features are reproducible and experiments done months apart show the existence of these features when exciting at wavelength III only, leading us to believe that these features are not derived from impurities in the vacuum chamber.

Feature III in the  $n = 1$  mass channel R2PI spectrum can be attributed solely to FL-H<sub>2</sub>O due to its absence in the  $n = 2$  mass channel spectrum. Therefore, the features in the RCS spectrum (1A) may be assigned to FL-H<sub>2</sub>O. The predominance of a similar but slightly different species of FL-H<sub>2</sub>O (1B) in trace II also indicates that feature II in the  $n = 1$  mass channel R2PI spectrum is primarily due to FL-H<sub>2</sub>O, although some contribution from FL-(H<sub>2</sub>O)<sub>2</sub> is evident.

Feature IV in both the  $n = 1, 2$  mass channel R2PI spectra is observed to appear with increasing intensity in the  $n = 1$  mass channel as the ionization energy is increased (i.e., one-color R2PI at  $33\,827.0\text{ cm}^{-1}$ ). This behavior is indicative of fragmentation of FL-(H<sub>2</sub>O)<sub>2</sub> into the  $n = 1$  mass channel,

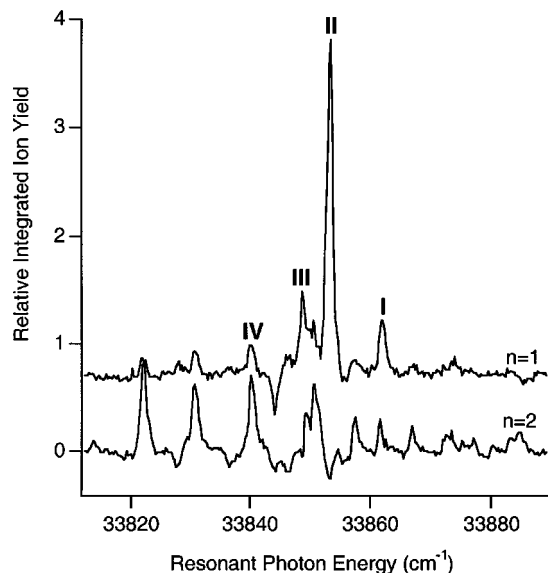


FIG. 5. Two-color R2PI spectra (ionization photon energy  $\sim 30\,800\text{ cm}^{-1}$ ) of fluorene- $(\text{D}_2\text{O})_n$ ,  $n = 1, 2$ .

and thus feature IV is attributed to  $\text{FL}-(\text{H}_2\text{O})_2$ . This assignment is consistent with rotational coherence trace IV, which is clearly due to a single species with a value of  $B+C$  distinct (15% difference) from the value of  $B+C$  for any of the  $\text{FL}-\text{H}_2\text{O}$  species. Finally, it can be concluded from the previous assignments that RCS trace I and feature I in the  $n=1$  mass channel R2PI spectrum are due to  $\text{FL}-\text{H}_2\text{O}$  and  $\text{FL}-(\text{H}_2\text{O})_2$  in approximately equal proportions. Rotational coherence traces I, II, and III show that multiple species can be identified in a polarized fluorescence decay curve without having to resort to kinetic models and fits.

$S_1$  lifetimes have been measured by orientation-independent (magic angle) fluorescence decay as an additional consistency check of the above-made assignments. Fluorescence decay curves were obtained over a time interval of 60 ns ( $\sim 5$  lifetimes) for excitation at energies I–IV. Distinct  $S_1$  lifetimes for the two states of  $\text{FL}-\text{H}_2\text{O}$  and for  $\text{FL}-(\text{H}_2\text{O})_2$  were obtained from single exponential fits to the fluorescence decay curves obtained at excitation energies II–IV. Analyses of the weighted residuals of both single exponential and biexponential fits to the decay curve obtained at excitation energy I indicate that it is biexponential. This is to be expected since rotational coherence trace I is clearly due to two different species in similar proportions. The two lifetimes obtained from the biexponential fit are the same as those obtained (within the experimental uncertainty) for  $\text{FL}-(\text{H}_2\text{O})_2$  and for version IA of  $\text{FL}-\text{H}_2\text{O}$ . The lifetime results are tabulated in Table I.

### B. $\text{FL}-(\text{D}_2\text{O})_{1,2}$ and $\text{FL}-\text{HDO}$

The two-color R2PI spectra (ionization photon energy  $\sim 30\,800\text{ cm}^{-1}$ ) of  $\text{FL}-(\text{D}_2\text{O})_{1,2}$  and  $\text{FL}-\text{HDO}$  are shown, respectively, in Figs. 5 and 6. As was done for  $\text{FL}-(\text{H}_2\text{O})_{1,2}$ , features in the R2PI spectra of  $\text{FL}-(\text{D}_2\text{O})_{1,2}$  have been assigned with the aid of the corresponding rotational coherence traces [the values of  $B+C$  for the species identified as

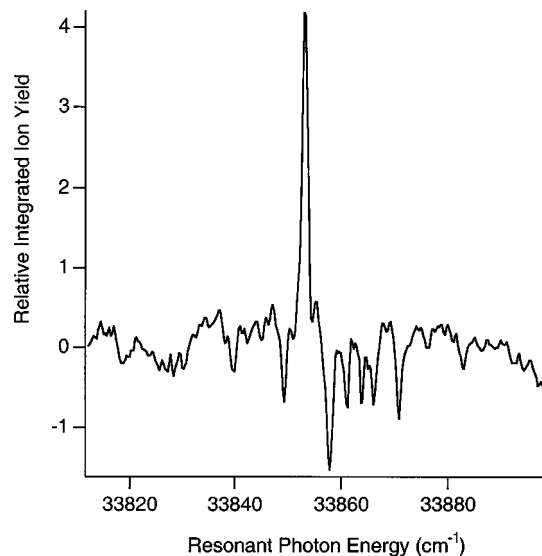


FIG. 6. Two-color R2PI spectrum (ionization photon energy  $\sim 30\,800\text{ cm}^{-1}$ ) of fluorene-HDO.

$\text{FL}-(\text{D}_2\text{O})_{1,2}$  are in Table I]. These assignments indicate that there is a one-to-one correspondence between features I, II, III in the  $\text{FL}-\text{D}_2\text{O}$  R2PI spectrum and features I, II, III in the  $\text{FL}-\text{H}_2\text{O}$  R2PI spectrum. It should be noted that while features II and III are present in the  $\text{FL}-\text{H}_2\text{O}$  and  $\text{FL}-\text{D}_2\text{O}$  R2PI spectra, only a single feature is observed in the  $\text{FL}-\text{HDO}$  spectrum. This point will be discussed further in Sec. IV B.

## IV. ANALYSIS AND DISCUSSION

### A. Determination of the structure of $\text{FL}-\text{H}_2\text{O}$ from the RCS data

Preliminary values of the excited state rotational constants  $A$ ,  $B$ ,  $C$  that are consistent with the values of  $B+C$  obtained from the RCS data are determined by guessing a physically reasonable cluster geometry and diagonalizing the moment of inertia tensor  $\mathbf{I}_{\mu\nu}$  (Refs. 33 and 34)

$$\mathbf{I}_{\mu\nu} = \begin{pmatrix} I_b + \mu(y^2 + z^2) & -\mu xy & -\mu xz \\ -\mu xy & I_a + \mu(x^2 + z^2) & -\mu yz \\ -\mu xz & -\mu yz & I_c + \mu(x^2 + y^2) \end{pmatrix} \quad (1)$$

subject to the constraint imposed by the measured value of  $B+C$ . In Eq. (1),  $I_b$ ,  $I_a$ ,  $I_c$  are the principal moments of inertia of bare fluorene,  $m$  is the reduced mass of the  $\text{FL}-\text{H}_2\text{O}$  system, and  $(x, y, z)$  is the position of the center of mass of the  $\text{H}_2\text{O}$  system in the coordinate system formed by the principal axes of bare fluorene (Fig. 1). The form of Eq. (1) treats the cluster as a pseudodiatom molecule and gives the position of the center of mass of the  $\text{H}_2\text{O}$  system in the principle axis system of fluorene. Since in the absence of  $C$ -type recurrences (at times  $n/4C$ ) only  $B+C$  is known, diagonalization of  $\mathbf{I}_{\mu\nu}$  is useful for determining preliminary

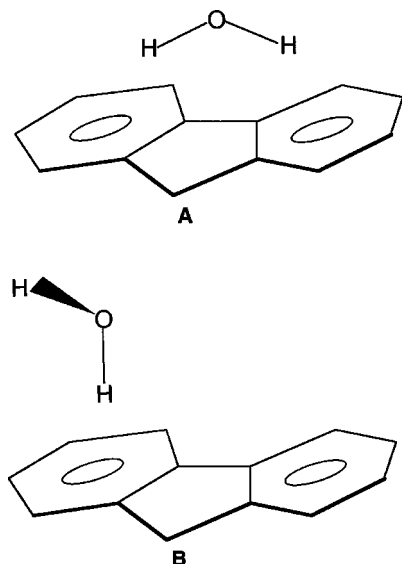


FIG. 7. Possible structures for fluorene-H<sub>2</sub>O. Structure A is the most likely structure.

values of  $A$ ,  $B$ ,  $C$  consistent with the measured value of  $B + C$  for use in the RCS simulations. Comparison of the RCS simulations to the observed experimental data then allow further refinement of the structure. Detailed theoretical treatments of RCS and methods for generating RCS simulations are available in the literature<sup>19</sup> and thus will not be discussed here. The parameters required for the simulations include the excited state rotational constants  $A$ ,  $B$ ,  $C$ , the direction cosines of the  $S_0 \rightarrow S_1$  transition moment in the principal axis system of the cluster, and the rotational temperature,  $T_{\text{rot}}$ , in the expansion. For the simulations shown in the following, the best agreement with the experimental rotational coherence traces was found for  $T_{\text{rot}} = 5$  K, and it was found in all cases that an  $a$  axis polarized  $S_1 \rightarrow S_0$  transition moment adequately simulated the experimental traces.

The RCS experiments demonstrate the existence of at least two distinct values of  $B + C$  for FL-H<sub>2</sub>O. Initial structure determinations were performed for species 1A as the experimental signal/noise is significantly higher in this case allowing for better structural determination of this species. Structures for FL-H<sub>2</sub>O with the water molecule centered over the central five-membered ring of fluorene (A) and with the water molecule over one of the six-membered aromatic sites (B) have been considered (Fig. 7). Our analysis is not sensitive to the positions of the hydrogens, only the center of mass of the H<sub>2</sub>O moiety may be determined. We have chosen to portray structure A as one in which both hydrogens bridge the central five-membered ring although a structure in which a single hydrogen bonds perpendicular to the five-membered ring would also be consistent with the experimental data. The RCS simulations corresponding to structure types A and B of FL-H<sub>2</sub>O (RCS trace II) are shown in Fig. 8 along with the experimental data. The experimental trace also shows some contribution from FL-(H<sub>2</sub>O)<sub>2</sub> as indicated. Both simulations accurately reproduce the dominant  $J$ -type transient spacing. However, structure B displays additional strong  $C$ -type transients not observed in the experimental trace. Such  $C$ -type

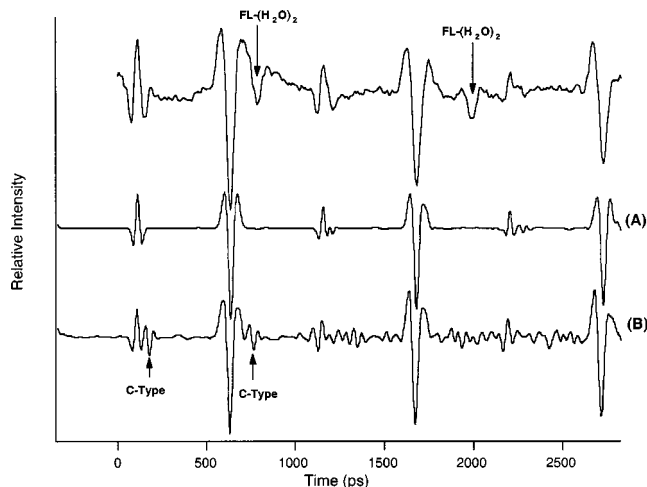


FIG. 8. Experimental RCS trace and RCS simulations for structures A and B of fluorene-H<sub>2</sub>O.

transients are indicative of the lower symmetry of structure B ( $k = -0.85$ ) compared to structure A ( $k = -0.93$ ). In addition, in order to correctly match the spacing of the  $J$ -type transients using structure B, the separation between the center of mass of the water molecule and the plane of the fluorene must be decreased to less than 2.2 Å. Here we are further guided by previous results on the benzene-H<sub>2</sub>O complex. The separation between the center of mass of the water molecule and the plane of the benzene ring in the benzene-H<sub>2</sub>O complex is  $\sim 3.3$  Å.<sup>7-9</sup> It is reasonable to expect that this separation would be similar in FL-H<sub>2</sub>O. Based on the observed benzene-H<sub>2</sub>O separation of  $\sim 3.3$  Å, a  $< 2.2$  Å separation in FL-H<sub>2</sub>O is physically unreasonable, corroborating our assignment that structure A is correct.

The coordinates of the center of mass of the water molecule in structure A for the simulation shown are  $(x, y, z) = (0.0 \text{ Å}, 0.0 \text{ Å}, 3.28 \text{ Å})$ , corresponding to excited state rotational constants  $A = 1.219$  GHz,  $B = 0.4922$  GHz,  $C = 0.4640$  GHz. The absence of obvious  $C$ -type recurrences in the rotational coherence trace is not surprising since a rotor with these rotational constants is very close to prolate symmetric (asymmetry parameter  $\kappa = -0.93$ ). This structure represents our best fit to the experimental data. Since only  $B + C$  is available from the data however, the structural parameters determined have some degree of uncertainty dependent on the experimental signal/noise. Using the above-determined structure, the expected value for  $B + C$  for FL-D<sub>2</sub>O is found to be 0.9480 GHz. This is consistent with the value observed experimentally.

## B. Determination of the structures of FL-(H<sub>2</sub>O)<sub>2</sub> from the RCS data

FL-(H<sub>2</sub>O)<sub>2</sub> can have two distinct configurations: either both waters attach to the same side of the planar fluorene molecule (2/0) or else one water resides above the rings with the other below (1/1). Both the 2/0 structure and the 1/1 structure can reproduce the measured RCS traces, as there are in effect too many degrees of freedom in this situation to allow a unique determination of the structure. However, the

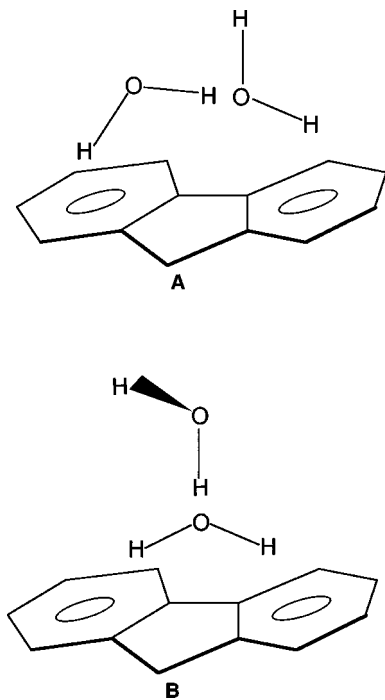


FIG. 9. Possible structures for fluorene-(H<sub>2</sub>O)<sub>2</sub>. Structure A is the most likely structure.

1/1 structure obtained by adding the second water molecule directly opposite the water molecule in FL-H<sub>2</sub>O does not reproduce the data. In addition, we expect that the 2/0 structure will be lowest in energy [as observed in benzene-(H<sub>2</sub>O)<sub>2</sub>—Ref. 9], since such a structure allows a stabilizing water-water interaction in addition to the two water-fluorene interactions. Thus, 1/1 type structures are not further considered here.

The structures considered for FL-(H<sub>2</sub>O)<sub>2</sub> are shown in Fig. 9, and the corresponding RCS simulations are shown in Fig. 10. In contrast to the case of FL-H<sub>2</sub>O, these simulations are performed assuming that the two waters form a hydrogen bonded dimer. The separation between the oxygen centers is assumed to be 2.75 Å as found in benzene-(H<sub>2</sub>O)<sub>2</sub>.<sup>9</sup> The FL-(H<sub>2</sub>O)<sub>2</sub> cluster may then be modeled as a

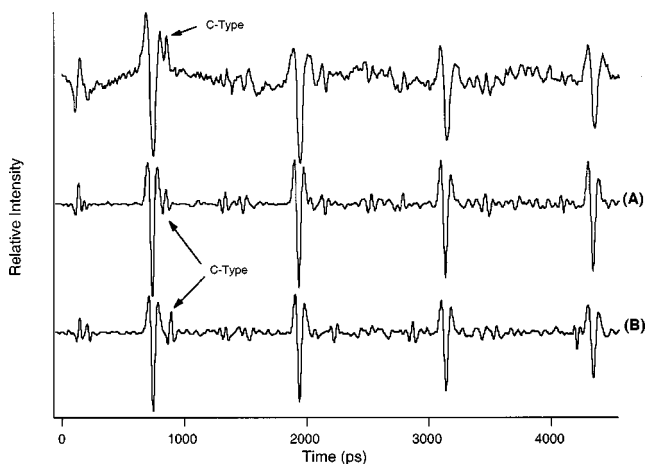


FIG. 10. Experimental RCS trace and RCS simulations for structures A and B of fluorene-(H<sub>2</sub>O)<sub>2</sub>.

diatomic molecule attached to bare fluorene. Once again, it is straightforward to write down the moment of inertia tensor in terms of the principal axes of the bare fluorene molecule. The RCS simulations shown in Fig. 10 demonstrate that structure A provides a better fit to the data than structure B. Structure B can reproduce the spacing of the *J*-type transients adequately, but the *C*-type transients then no longer display the correct positions. Simulations such as that shown in A imply that the water dimer lies flat or close to flat along the long axis above the fluorene ring. The coordinates of the first water molecule in structure A for the simulation shown are  $(x,y,z) = (-0.73 \text{ \AA}, -1.38 \text{ \AA}, 3.47 \text{ \AA})$  while the second water of the dimer is located at  $(-0.73 \text{ \AA}, 1.37 \text{ \AA}, 3.47 \text{ \AA})$ . This leads to excited state rotational constants of  $A = 0.8260$ ,  $B = 0.4457$ , and  $C = 0.3841$ . Even given the added constraint required by the *C*-type transients in the RCS traces, defining a unique structure is problematic. We emphasize that there are other structures that are consistent with the observed RCS traces. At present we are only able to rule out structures such as B where both water molecules are atop the same point of the fluorene plane. Assuming the structure above, we find that the value of  $B + C$  for FL-(D<sub>2</sub>O)<sub>2</sub> to be 0.8151, consistent with that observed experimentally.

### C. Internal rotation of the water molecule in FL-H<sub>2</sub>O/D<sub>2</sub>O/HDO

Doublet structures for the  $6_0^1$  transitions of benzene-H<sub>2</sub>O/D<sub>2</sub>O (R2PI) have been observed and associated with transitions from both the  $m=0$  and  $m=\pm 1$  ground state internal rotation levels (where  $m$  is the internal rotation quantum number, selection rule:  $\Delta m=0$ ), both of which remain populated in the jet because cooling from  $m=\pm 1$  to  $m=0$  is inhibited due to the different nuclear spin symmetries of the  $m=0$  and  $m=\pm 1$  levels.<sup>7-9</sup> If the rotational barrier or average geometry of the complex changes upon electronic excitation, the difference in energy between the  $m=0$  and  $m=\pm 1$  levels will be different in the ground and excited states, and thus the  $m=0 \rightarrow m'=0$  and  $m=\pm 1 \rightarrow m'=\pm 1$  transitions will occur at different energies. Cooling from  $m=\pm 1$  to  $m=0$  is not inhibited in benzene-HDO due to the lack of nuclear spin symmetry restrictions, and thus only a single  $6_0^1$  transition from the  $m=0$  rotorsional level is observed.

As in the case of benzene-H<sub>2</sub>O/D<sub>2</sub>O/HDO, the presence of the doublet (II, III) in the FL-H<sub>2</sub>O and FL-D<sub>2</sub>O R2PI spectra, and its absence in the FL-HDO R2PI spectrum, indicate internal rotation of the water molecule. Features II, III in the FL-H<sub>2</sub>O/D<sub>2</sub>O spectra are both assigned to the  $0_0^0$  transition, which is split due to transitions from both the  $m=0$  and  $m=\pm 1$  ground state internal rotation levels. The single feature in the FL-HDO spectrum is assigned to the  $0_0^0$  transition from the  $m=0$  internal rotation level.

The redshifted and blueshifted features in the  $6_0^1$  transition of benzene-H<sub>2</sub>O have been assigned, respectively, to  $m=\pm 1 \rightarrow m'=\pm 1$  and  $m=0 \rightarrow m'=0$  based on a slight decrease in the intensity of the redshifted feature relative to the blueshifted feature when the backing pressure of the jet is increased.<sup>9</sup> It is felt that the R2PI apparatus used in the current study is not sufficiently stable to make any conclusions



about slight changes in R2PI intensities with backing pressure, and thus it is not possible to reliably assign R2PI features II and III to the  $m = \pm 1 \rightarrow m' = \pm 1$  or  $m = 0 \rightarrow m' = 0$  transitions. The fact that the lifetime corresponding to the redshifted feature is longer than that of the blueshifted feature (Table I) suggests that the excited state level of the redshifted feature is lower in energy, i.e., the density of states decreases with decreasing energy, therefore the rate of radiationless decay is lower and the lifetime is longer. As such, the redshifted feature is tentatively assigned to the  $m = 0 \rightarrow m' = 0$  transition since the  $m' = 0$  level is lower in energy than the  $m' = \pm 1$  level.

The recurrences in RCS trace II (1B) have a different value of  $B + C$  and decay slower than the recurrences in trace III (1A). It is possible then that the two different internal rotation levels result in two different sets of recurrences. Significant variations of rotational recurrence *decay* rates, although not recurrence times, have been observed for different torsional levels of rotors with internally rotating subunits.<sup>35</sup> This variation in rotational recurrence decay rate has been attributed to the dependence of the rotational constants, and hence the asymmetry of the rotor, on the torsional level. This effect, however, was observed for internal rotation of the relatively massive anthryl subunits of 9,9'-bianthryl, and it seems unlikely that rotation of the water molecule about its twofold axis will introduce a similar observable dependence of the asymmetry of the rotor on the internal rotation level. Finally, centrifugal distortion will decrease the amplitudes of rotational recurrences, however, centrifugal distortion is expected to be minimal in samples with low rotational temperatures.<sup>27</sup>

## V. CONCLUSION

The  $S_1$  structures of FL-H<sub>2</sub>O and FL-(H<sub>2</sub>O)<sub>1,2</sub> have been elucidated by RCS via time-resolved polarized fluorescence. FL-H<sub>2</sub>O has a structure in which the oxygen atom lies above the central five-member ring most likely with both hydrogens interacting with the aromatic sites of fluorene. In FL-(H<sub>2</sub>O)<sub>2</sub>, the water molecules form a dimer that is likely oriented above the long axis of fluorene and is hydrogen-bonded, via both water molecules, to both aromatic sites.

Evidence of internal rotation of the water molecule is present in the R2PI spectra of FL-H<sub>2</sub>O/D<sub>2</sub>O/HDO. This internal rotation appears to manifest itself in the rotational coherence traces as a dependence of the spacing and decay rates of the rotational recurrences on the internal rotation level. RCS experiments are under way to determine how the hydrogen bonding patterns and rotational recurrence widths and decay rates seen in fluorene-water complexes differ from those of complexes of fluorene with other hydrogen bonding species.

## ACKNOWLEDGMENTS

We would like to thank Professor Peter Felker for generously providing the simulation algorithm developed by his research group and for helpful comments. This work was

supported by the U.S. Department of Energy Office of Basic Energy Sciences, Chemical Sciences Division, and it was performed at the W. R. Wiley Environmental Molecular Sciences Laboratory, a national scientific user facility sponsored by the Department of Energy's Office of Biological and Environmental Research and located at Pacific Northwest National Laboratory. Pacific Northwest National Laboratory is operated for the U.S. Department of Energy by Battelle under Contract No. DE-AC06-76RLO 1830.

- <sup>1</sup>C. J. Gruenloh, J. R. Carney, F. C. Hagemester, T. S. Zwier, S. Y. Fredericks, J. T. Wood III, and K. D. Jordan, *J. Chem. Phys.* **109**, 6601 (1998).
- <sup>2</sup>P. M. Maxton, M. W. Schaeffer, and P. M. Felker, *Chem. Phys. Lett.* **241**, 603 (1995).
- <sup>3</sup>R. N. Pribble and T. S. Zwier, *Science* **265**, 75 (1994).
- <sup>4</sup>R. N. Pribble and T. S. Zwier, *Faraday Discuss.* **97**, 229 (1994).
- <sup>5</sup>R. N. Pribble, A. W. Garret, K. Haber, and T. S. Zwier, *J. Chem. Phys.* **103**, 531 (1995).
- <sup>6</sup>B.-M. Cheng, J. R. Grover, and E. A. Walters, *Chem. Phys. Lett.* **232**, 364 (1995).
- <sup>7</sup>H. S. Gutowsky, T. Emilsson, and E. Arunan, *J. Chem. Phys.* **99**, 4883 (1993).
- <sup>8</sup>S. Suzuki, P. G. Green, R. E. Bumgarner, S. Dasgupta, W. A. Goddard III, and G. A. Blake, *Science* **257**, 942 (1992).
- <sup>9</sup>A. J. Gotch and T. S. Zwier, *J. Chem. Phys.* **96**, 3388 (1992).
- <sup>10</sup>A. W. Garrett and T. S. Zwier, *J. Chem. Phys.* **96**, 3402 (1992).
- <sup>11</sup>A. J. Gotch, A. W. Garrett, D. L. Severance, and T. S. Zwier, *Chem. Phys. Lett.* **178**, 121 (1991).
- <sup>12</sup>D. Feller, *J. Phys. Chem.* **103**, 7558 (1999).
- <sup>13</sup>P. Tarakeshwar, H. S. Choi, S. J. Lee, J. Y. Lee, K. S. Kim, T.-K. Ha, J. H. Jang, J. G. Lee, and H. Lee, *J. Chem. Phys.* **111**, 5838 (1999).
- <sup>14</sup>S. Y. Fredericks, K. D. Jordan, and T. S. Zwier, *J. Phys. Chem.* **100**, 7810 (1996).
- <sup>15</sup>J. K. Gregory and D. C. Clary, *Mol. Phys.* **88**, 33 (1996).
- <sup>16</sup>J. D. Augspurger, C. E. Dykstra, and T. S. Zwier, *J. Phys. Chem.* **96**, 7252 (1992).
- <sup>17</sup>T. Troxler, B. A. Pryor, and M. R. Topp, *Chem. Phys. Lett.* **239**, 44 (1995).
- <sup>18</sup>P. M. Andrews, B. A. Pryor, M. B. Berger, P. M. Palmer, and M. R. Topp, *J. Phys. Chem.* **101**, 6222 (1997).
- <sup>19</sup>P. M. Felker and A. H. Zewail, *J. Chem. Phys.* **86**, 2460 (1987).
- <sup>20</sup>J. S. Baskin, P. M. Felker, and A. H. Zewail, *J. Chem. Phys.* **86**, 2483 (1987).
- <sup>21</sup>P. Benharash, M. J. Gleason, and P. M. Felker, *J. Phys. Chem. A* **103**, 1442 (1999).
- <sup>22</sup>C. Riehn, A. Weichert, M. Zimmerman, and B. Brutschy, *Chem. Phys. Lett.* **299**, 103 (1999).
- <sup>23</sup>T. Troxler, M. R. Topp, B. S. Metzger, and L. H. Spangler, *Chem. Phys. Lett.* **238**, 313 (1995).
- <sup>24</sup>T. Troxler, J. R. Stratton, P. G. Smith, and M. R. Topp, *Chem. Phys. Lett.* **222**, 250 (1994).
- <sup>25</sup>J. R. Stratton, T. Troxler, B. A. Pryor, P. G. Smith, and M. R. Topp, *J. Phys. Chem.* **99**, 1424 (1995).
- <sup>26</sup>T. Troxler, P. G. Smith, and M. R. Topp, *Chem. Phys. Lett.* **211**, 371 (1993).
- <sup>27</sup>P. M. Felker, *J. Phys. Chem.* **96**, 7844 (1992), and citations within.
- <sup>28</sup>A. R. Auty, A. C. Jones, and D. Phillips, *J. Chem. Soc., Faraday Trans. 2* **82**, 1219 (1986).
- <sup>29</sup>H. S. Im, V. H. Grassian, and E. R. Bernstein, *J. Phys. Chem.* **94**, 222 (1990).
- <sup>30</sup>U. Even and J. Jortner, *J. Chem. Phys.* **78**, 3445 (1983).
- <sup>31</sup>R. Knochenmuss, D. Ray, and W. P. Hess, *J. Chem. Phys.* **100**, 44 (1994).
- <sup>32</sup>P. W. Joireman, L. L. Connell, S. M. Ohline, and P. M. Felker, *J. Chem. Phys.* **96**, 4118 (1992).
- <sup>33</sup>W. Gordy and R. L. Cook, *Microwave Molecular Spectra* (Wiley-Interscience, New York, 1984).
- <sup>34</sup>W. L. Meerts, W. A. Majewski, and W. M. van Herpen, *Can. J. Phys.* **62**, 1293 (1984).
- <sup>35</sup>T. Fujiwara, Y. Fujimura, and O. Kajimoto, *Chem. Phys. Lett.* **261**, 201 (1996).